

Diffusion-limited dissolution of spherical particles
A critical evaluation and applications of approximate solutions

Guo, Xiaoling; Sietsma, Jilt; Yang, Yongxiang; Sun, Zhi; Guo, Muxing

DOI

[10.1002/aic.15676](https://doi.org/10.1002/aic.15676)

Publication date

2017

Document Version

Final published version

Published in

AICHE Journal

Citation (APA)

Guo, X., Sietsma, J., Yang, Y., Sun, Z., & Guo, M. (2017). Diffusion-limited dissolution of spherical particles: A critical evaluation and applications of approximate solutions. *AICHE Journal*, 63(7), 2926-2934. <https://doi.org/10.1002/aic.15676>

Important note

To cite this publication, please use the final published version (if applicable). Please check the document version above.

Copyright

Other than for strictly personal use, it is not permitted to download, forward or distribute the text or part of it, without the consent of the author(s) and/or copyright holder(s), unless the work is under an open content license such as Creative Commons.

Takedown policy

Please contact us and provide details if you believe this document breaches copyrights. We will remove access to the work immediately and investigate your claim.

Diffusion-Limited Dissolution of Spherical Particles: A Critical Evaluation and Applications of Approximate Solutions

Xiaoling Guo, Jilt Sietsma, and Yongxiang Yang

Dept. of Materials Science and Engineering, Delft University of Technology, Mekelweg 2, Delft 2628 CD, the Netherlands

Zhi Sun

Dept. of Materials Science and Engineering, Delft University of Technology, Mekelweg 2, Delft 2628 CD, the Netherlands

National Engineering Laboratory for Hydrometallurgical Cleaner Production Technology, Institute of Process Engineering, Chinese Academy of Sciences, Beijing 100190, China

Muxing Guo

Dept. of Materials Engineering, KU Leuven, Kasteelpark Arenberg 44 - box 2450, Leuven 3001, Belgium

DOI 10.1002/aic.15676

Published online February 22, 2017 in Wiley Online Library (wileyonlinelibrary.com)

The analytical and numerical description of the effective dissolution kinetics of spherical particles into a solvent is often difficult in chemical and metallurgical engineering. The crucial first step is to identify the dissolution mechanisms, and subsequently, relevant kinetics parameters can be calculated. In this article, three frequently used approximations, i.e., the invariant-field (IF) (Laplace), reverse-growth (RG), and invariant-size (IS) (stationary-interface) approximations, are systematically discussed and compared with numerical simulation results. The relative errors of the dissolution curves and total dissolution time of the three approximations to the numerical simulations are calculated. The results reveal the appropriate application ranges of the approximations for given precision levels. With further experimental validation, this research provides a methodology to properly assess dissolution kinetics and adequately estimate effective diffusion coefficients and activation energy under the experimental uncertainties. © 2017 American Institute of Chemical Engineers AICHE J, 63: 2926–2934, 2017

Keywords: diffusion-limited dissolution, kinetics, invariant-field approximation, reverse-growth approximation, invariant-size approximation

Introduction

Dissolution is a process of dissolving gases, liquids, or solids into a solvent and is a phenomenon widely occurring in the field of chemical and metallurgical engineering, such as precipitate dissolution during the heat treatment of steels,¹ drug release from solid pharmaceutical dosage forms,² dissolution of fluxes in metallurgical processes,³ etc. One of the most important aspects of dissolution is the kinetics, with which the rate-limiting step(s), as well as relevant kinetics parameters, can be identified.⁴ In a stagnant fluid or solid, dissolution rate can be controlled either by the diffusion of solute atoms or molecules in the matrix, or the interface reaction that transfers atoms or molecules across the phase interface.⁵

For diffusion-limited dissolution, the concentration field can be described using Fick's second law. However, an exact analytical solution is only possible for planar particles or precipitates.⁶ For spherical ones, several approximate analyses have

been suggested to simplify the mathematics.⁶ The invariant-field (IF) (Laplace), reverse-growth (RG), and invariant-size (IS) (stationary-interface) approximations are three frequently used approximate methods. Due to the lack of an exact analytical solution, their accuracy and applicable ranges have hardly been evaluated systematically and quantitatively in the literature.⁶ However, when these approximations are applied to academic research, their accuracy is of the first order of importance. Otherwise, the reliability of the results (e.g., derived physiochemical parameters—diffusion coefficients) is not clear and conclusions may be misleading. With the aids of computer technology, the diffusion equations were solved numerically.^{5,7–12} The numerical solutions should be considered to be more accurate than analytical approximations as they take into account the effects of the moving boundary and the resulting radial convective transport, which are ignored in approximate methods.^{6–8} Even though the numerical simulations can produce more reliable solutions than analytical solutions, it needs considerable efforts and time to build a proper model. An appropriate analytical approximation can be very efficient as long as the errors can be controlled under the desired levels.

Correspondence concerning this article should be addressed to X. Guo at x.guo-1@tudelft.nl and to Z. Sun at zhisun@126.com.

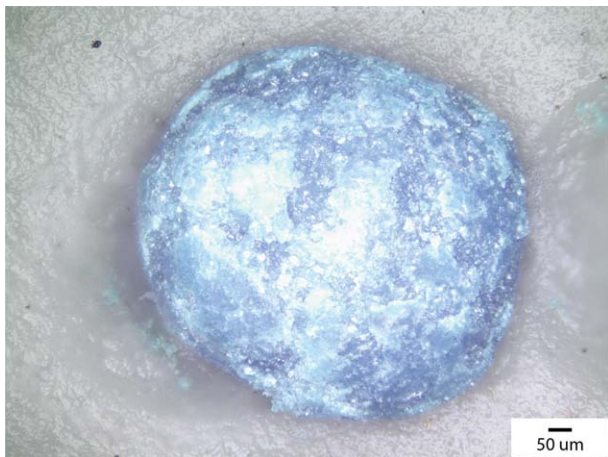


Figure 1. Quasi-spherical Nd_2O_3 particle for CSLM experiments.

[Color figure can be viewed at wileyonlinelibrary.com]

Confocal scanning laser microscope (CSLM) can provide an *in situ* observation of physicochemical phenomena at high temperatures. This advanced technique has been applied to studying various dissolution phenomena in metallurgical processes.^{13–16} In this article, the theory is validated with experimental results obtained with CSLM.

This research is carried out in accordance with the significance of systematic evaluation of approximate methods to validate their applicability. Three approximations, i.e., IF, RG, and IS approximations, are considered and compared with numerical simulations. This article presents a full picture of the accuracy of the three approximations in terms of a physicochemical parameter, k . The outcome can be served as a guideline for the applications in the scientific field. With a systematically understanding of the features of the IF, RG, and IS approximations, their feasibility for dissolution kinetics is assessed with experimental results. Two examples with diverse values of the physicochemical parameter are given. One example is taken from our previous work, studying the dissolution behavior of alumina particles in a $\text{CaO-Al}_2\text{O}_3\text{-SiO}_2$ melt.¹⁵ This research also provided numerical simulation results, which will give strong support to the present work with direct comparison with approximate solutions. The other is from the present work—the dissolution of Nd_2O_3 particles in $\text{LiF-24 (mol \%)} \text{CaF}_2$.

Experimental Procedure

Materials

The Nd_2O_3 particles were made of Nd_2O_3 powder with a purity of 99.95 wt % (produced by Alfa Aesar). The Nd_2O_3 powder was compressed into small cylinders with both a diameter and a height of ca. 2 mm by cold isostatic pressing. The cylinders were sintered in a box furnace, which was heated up to 1773 K at the rate of 1 K per minute, then kept for 3 hours, and cooled down to room temperature at the rate of 5 K per minute. After sintering, the apparent density was measured to be on average of 6.8 g/cm^3 by the Archimedes' method (vs. true density of Nd_2O_3 7.24 g/cm^3 ¹⁷ and melt density $2.1\sim 2.0 \text{ g/cm}^3$ at $1141\sim 1291 \text{ K}$ calculated according to Ref. 18). The cylinders were rounded and downsized to quasi-spherical particles with a diameter of a few hundred micrometers in an in-house designed vessel, where the particles

were continuously blown by compressed air and collided with the steel wall of the apparatus. An image of a prepared Nd_2O_3 particle is shown in Figure 1.

LiF and CaF_2 used in the experiments were from Alfa Aesar, both with purities of 99.95 wt %. The pure compounds were blended manually based on their ratio in the desired melt, LiF-24CaF_2 . The well-mixed powders were then held in graphite crucibles, which were heated in a horizontal furnace to 50 K above the melting point of the mixtures ($T_m = 1023 \text{ K}$) and kept for at least 2 hours to homogenize. After the pre-melting, the master salts were quenched with liquid nitrogen in a stainless steel container and crushed into small pieces for the subsequent experiments using CSLM.

Experimental equipment and procedures

The dissolution of Nd_2O_3 particles in LiF-24CaF_2 melt was observed *in situ* with CSLM-IIF (CSLM, Lasertec, 1LM21M-SVF17SP). A detailed description of CSLM was given in our previous work.¹⁶ The temperature was measured by a B-type thermocouple (Pt-30 (wt %) Rh/Pt-6Rh) welded at the bottom of the sample holder. The uncertainty of the temperature measurement is $\pm 2 \text{ K}$. The HiTOS software connected to a REX-P300 controller is used to program temperature profiles. To ensure the accuracy of the experimental temperature, calibration was performed using standard pure metals, i.e., copper, nickel, palladium, and iron. The results show that the real temperature is 18 K higher than the measurement in the temperature range of this study. The temperatures will be presented as the measured values plus 18 K, the best estimate of the real temperature.

The procedure of CSLM experiments was described in another Ref. 16. In this investigation, the dissolution experiments were performed at 1141, 1191, 1241, and 1291 K. The dissolution processes were recorded in images with the HiTOS software at a rate of one frame per second. As shown in Figure 1, the particles used in the experiments were not perfectly spherical. Numerical simulations¹⁹ indicated that the dissolution time for a given shape of precipitate is the same as that for a sphere of the same cross-sectional area. Therefore, the equivalent radius should be used when solutions derived from spheres are applied in the analysis. To do so, a border was constructed around the particle using image processing software, ImageJ, as shown in Figure 2. An equivalent radius was calculated based on the measured 2D area of the particle. To minimize the systematic error in generating the borders, this procedure was repeated three times for each image and the average radius was later used in the kinetics study.

Approximate Solutions for Dissolution of a Single Particle in an Infinite Medium

General assumptions and equations

To consider the general problem of the diffusion-limited dissolution of a spherical particle with original radius, R_0 , in an infinite medium (Figure 3), several assumptions were made for simplifying geometrical and dissolution conditions:

1. The dissolution occurs at a sharp interface between the particle and medium, and equilibrium is obtained at the interface.
2. There are no solid products formed surrounding the particle during dissolution, i.e., the substance of the particle dissolves directly in the medium.

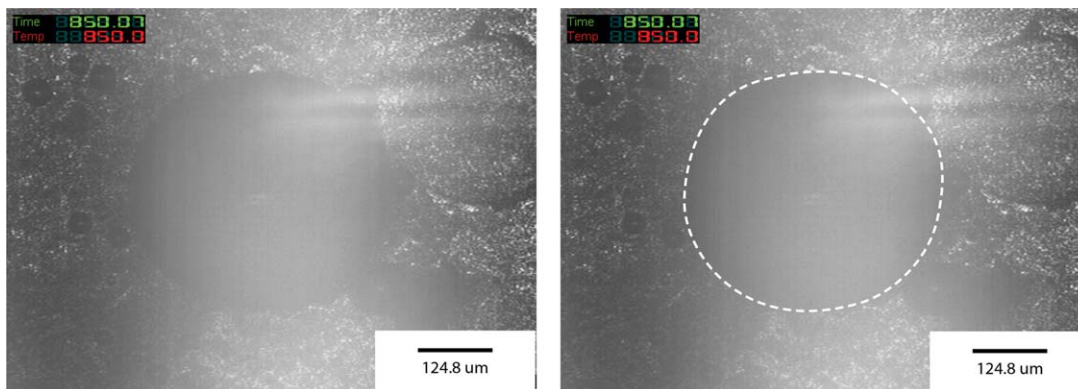


Figure 2. Illustration of processing CSLM images.

[Color figure can be viewed at wileyonlinelibrary.com]

3. The particle consists of pure substance and is homogeneous, i.e., the composition of the particle, C_P , is considered to be constant, and is independent of the radial distance, r , from the center of the particle, and time, t .

4. The effective diffusion coefficient, D , is used to describe the complex interdiffusion of particle atoms/molecules in the solution, i.e., a multicomponent system is treated as a quasi-binary system of the solute and medium. In the scope of this article, it is reasonable to assume the diffusion coefficient to be independent of composition and only a function of temperature, T .¹²

5. Assuming that the medium is infinite, the far-field composition of the matrix, C_M , remains constant throughout the dissolution process.

6. The concentration profile around the particle is spherically symmetric, which means that the concentration of particle atoms/molecules in the solution, C , is a function of r and t , while the particle radius, R , is a function of time only (see Figure 3).

7. Curvature and strain effects are ignored as they are found to be small and negligible in the cases concerned.⁵

8. The partial specific volume of each component does not vary with the composition of the solution.

For the diffusion-controlled dissolution of an isolated sphere in an infinite matrix, the concentration field follows Fick's second law

$$D \left(\frac{\partial^2 C}{\partial r^2} + \frac{2}{r} \frac{\partial C}{\partial r} \right) = \frac{\partial C}{\partial t} \quad (1)$$

which satisfies the following boundary conditions

$$C(r=R, 0 < t \leq \infty) = C_I$$

$$C(r > R, t=0) = C_M \quad (2)$$

$$C(r=\infty, 0 \leq t \leq \infty) = C_M$$

where C_I is the equilibrium concentration of the solute at the interface. At the interface, the flux balance should be maintained via

$$(C_P - C_I) \frac{dR}{dt} = D \left(\frac{\partial C}{\partial r} \right) \Big|_{r=R} \quad (3)$$

The concentration field varies with time due to the diffusion of solute (Eq. 1) and the interface motion (Eq. 3). An exact analytical solution with respect to spherical particles has not yet been available.⁶ Several approximate analyses, e.g., the IF, RG, and IS approximations, were derived.⁶ Meanwhile, numerical solutions were also proposed.^{5,7-12} In the following sections, more details about the analytical approximations will be given and their accuracy will be discussed by comparing with numerical solutions.

IF (Laplace) approximation

The IF approximation treats the dissolution as a quasi-equilibrium process. The concentration profile is independent of time, which implies that the interface is fixed at R_0 . This method solves the simpler resulting Laplace equation $\nabla^2 C = 0$ by setting $\partial C / \partial t = 0$ rather than Eq. 1. The solution is⁶

$$C = C_M + \frac{(C_I - C_M)R}{r} \quad (4)$$

For simplification, the following parameter is defined as dimensionless time

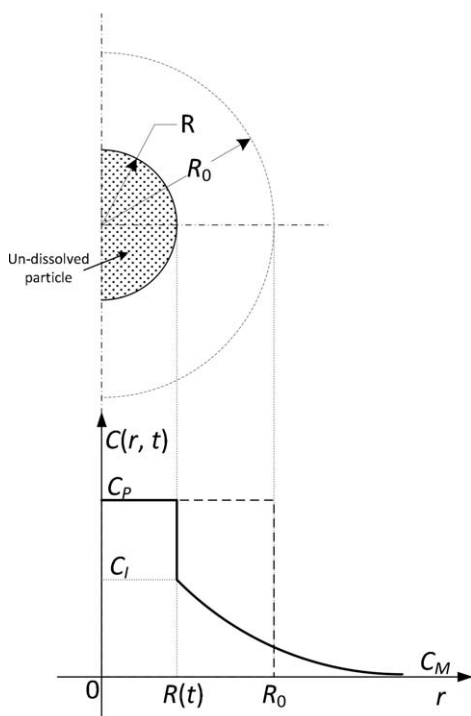


Figure 3. Illustration of concentration profile of solute atoms/molecules in matrix.

$$t' = \frac{kDt}{R_0^2} \quad (5)$$

where

$$k \equiv \frac{2(C_I - C_M)}{C_P - C_I} \quad (6)$$

The physicochemical parameter, k , is related to the supersaturation ratio and is a measure of the driving force for diffusion, varying from zero to positive infinity. Small k means weak driving force, which leads to low dissolution rate. Similarly, large k suggests fast dissolution. k is a crucial parameter in this article and its value will be used to define the applicable ranges of different approximations.

Therefore, the dimensionless time of complete dissolution is

$$t'_0 \equiv \frac{kD\tau}{R_0^2} \quad (7)$$

where τ is the time for complete dissolution. On substitution of Eqs. 4 to 7 into Eq. 3 and integrating, the evolution of particle radius is given as

$$y^2 = 1 - t' \quad (8)$$

Or

$$y^2 = 1 - \frac{t}{\tau_{IF}} \quad (9)$$

where y is the ratio of the actual particle radius to the original one, R/R_0 , and the subscript, IF, indicates that the theoretical total dissolution time is given by the IF approximation and hereafter similarly for other approximations. The total dissolution time can be calculated via

$$\tau_{IF} = \frac{R_0^2}{kD} \quad (10)$$

RG approximation

If the dissolution is treated as essentially the reverse of growth, the concentration field will be⁶

$$C = C_M + A \left[\frac{\sqrt{D(\tau-t)}}{r} \exp\left(\frac{-r^2}{4D(\tau-t)}\right) - \frac{\sqrt{\pi}}{2} \operatorname{erfc}\left(\frac{r}{2\sqrt{D(\tau-t)}}\right) \right] \quad (11)$$

where

$$A = \frac{2\lambda_R(C_I - C_M)}{\exp(-\lambda_R^2) - \pi^{1/2}\lambda_R \operatorname{erfc}(\lambda_R)} \quad (12)$$

and λ_R is given as

$$\lambda_R^2 \exp(\lambda_R^2) \left[\exp(-\lambda_R^2) - \pi^{1/2}\lambda_R \operatorname{erfc}(\lambda_R) \right] = \frac{k}{4} \quad (13)$$

There is only one positive value of λ_R that satisfies Eq. 13. Since the solution is deduced from the concentration field of spheres growing from zero to R_0 , Eq. 11 does not satisfy Eq. 1 and not all the boundary conditions, i.e., $C(r > R, t=0) \neq C_M$. The gradient surrounding the particle at time zero is not infinite. With these deviations, the exact solution for growth turns out to be an approximation for dissolution.

The relationship between the particle radius and dissolution time is

$$y^2 = 1 - \frac{t}{\tau_{RG}} \quad (14)$$

with

$$\tau_{RG} = \frac{R_0^2}{4\lambda_R^2 D} \quad (15)$$

IS (stationary interface) approximation

The IS approximation neglects the effect of the interface motion. The interface is assumed to be fixed at R_0 from the start of dissolution as the movement of the interface is relatively small and is considered negligible compared to the width of the diffusion field for slow dissolution. Unlike the IF approximation, the concentration field varies with time and IS approximation takes into account the influence of transience before steady state. The concentration profile is²⁰

$$C = C_M + \frac{(C_I - C_M)R}{r} \operatorname{erfc}\left(\frac{r-R}{2\sqrt{Dt}}\right) \quad (16)$$

Substituting into Eq. 3,

$$\frac{dR}{dt} = -\frac{kD}{2R} - \frac{k}{2} \sqrt{\frac{D}{\pi t}} \quad (17)$$

or

$$\frac{dy}{dt} = -\frac{1}{2y} - \frac{p}{\sqrt{t'}} \quad (18)$$

where

$$p^2 = \frac{k}{4\pi} \quad (19)$$

An implicit relation was obtained for y as a function of t' .²⁰

$$\ln\left(y^2 + 2pt'^{1/2}y + t'\right) = \frac{-2p}{(1-p^2)^{1/2}} \arctan\left[\frac{(1-p^2)^{1/2}}{y/t'^{1/2} + p}\right] \quad (20)$$

with

$$\tau_{IS} = \frac{R_0^2}{kD \exp\left\{\frac{2p}{(1-p^2)^{1/2}} \arctan\left[\frac{(1-p^2)^{1/2}}{p}\right]\right\}} \quad (21)$$

It should be mentioned that Eq. 20 with p equal zero will reduce to Eq. 8. When the driving force is approaching zero, the transient period disappears and the dissolution becomes a steady-state process.

Results and Discussion

Evaluation of approximations

Due to the lack of an exact analytical solution for the dissolution of spherical particles, the accuracy of the various approximations is studied by comparison with numerical results. The latter is considered to be more precise than approximate methods because the numerical simulations take into account the influence of moving interface during dissolution,^{8,10,12} which is difficult to be considered in analytical approximations. The results from Ref. 12 are used in this

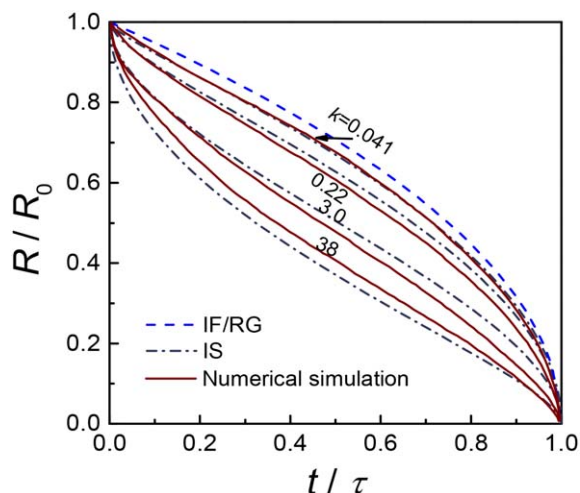


Figure 4. Comparison of various approximations with numerical results from Ref. 12.

[Color figure can be viewed at wileyonlinelibrary.com]

article as it presents data in such a way that the total dissolution time and radius-time relationships can be obtained for a wide range of k with little further computation.

Figure 4 shows the variation of the normalized radius with relative time for numerical results up to $k = 38$ with solid lines.¹² In general, the rate of dissolution (the slope of the curve) initially decreases with time and increases again at a later stage. In the first place, the decrease in dissolution rate arises from the sharp decrease in the concentration gradient at the interface from its original infinite value when the solute concentration near the interface increases. Comparing the curves with various k values, it is obvious that the shape of the curves depends on k and the curves with large k exhibit higher dissolution rate at the early stage than those with small k values.

By further comparing the aforementioned approximations with the numerical results (Figure 4), the differences among different approximations can be identified. The curves of IF and RG are the same (Eqs. 9 and 14) and remain unchanged with varying k values, while those of the IS approximation varies with k values. Obviously, the IS approximation yields a radius-time relationship that has a rather good agreement with the numerical simulation results. The approximation is almost the same as the numerical results for $k = 0.041$. This small k value means that the concentration difference between the particle and the interface is much higher than that between the interface and the matrix. This guarantees the movement of the interface to be slow and the interface is approximately fixed compared to the scale of the diffusion field. The error introduced, therefore, is negligible, and the deviation between the IS approximation and numerical results is extremely small (Figure 4). As mentioned previously, IF can be viewed as the extreme condition of IS, i.e., $p = 0$ or $k = 0$. This is clearly illustrated in Figure 4. The difference between IS and IF decreases with k values and IS will coincide with IF eventually when k is approaching zero.

The average relative errors of the approximations to the numerical simulations were calculated to compare the dissolution curves quantitatively. The values were averaged over 50 points that are evenly distributed between zero and one. The results are shown in Figure 5. In the range of k from 0 up to 38, the maximum error of IS is below 8%. Compared with IS,

the errors of IF or RG are always higher (Figure 5). The deviation increases sharply with k values, as also clearly seen from Figure 4. This suggests that the dissolution curves of IF or RG would differ substantially from the experimental results with large k , e.g., the deviation is as large as 50% for $k = 10$. Figure 5 can be used to identify the applicable range of each approximation for a given error level. For example, if the experimental uncertainty is around 10%, IF or RG can only be applied to those with $k < 0.09$ to ensure the error introduced below the experimental deviation while IS will be feasible for k up to 38 as its relative error is always lower than 8%. From this point of view, IS is a better method than IF or RG. For those with $k < 0.09$, IF or RG could be a better method to identify whether a process is diffusion-controlled as it is easy to derive the dissolution curve without knowing any physiochemical property of the studied system as k is not necessarily needed (Eqs. 9 and 14).

To compare the total dissolution time estimated by the approximations and numerical simulations, it is convenient to introduce another dimensionless total dissolution time, defined by

$$t_0^* \equiv \frac{D\tau}{R_0^2} \quad (22)$$

Figure 6 compares the variation of t_0^* with k values obtained via the approximations and numerical simulation. In general, the total dissolution time decreases with increasing k . Dissolution is enhanced for large k , resulting in short dissolution time. The total dissolution times calculated by the three approximations are very similar in the limit of small k and all the approximations yield rather good agreement with the numerical method. The approximations, however, deviate from the numerical simulation gradually with increasing k . The complete dissolution time calculated from the IS approximation is almost half of the one obtained from the numerical solution at $k = 2$. Meanwhile, the values given by the IS approximation are always smaller than those from the numerical simulation (Figure 6). This means that the IS approximation tends to overestimate the dissolution kinetics due to the negligence of boundary motion, resulting in the calculated concentration gradient at the interface is steeper than the real one.

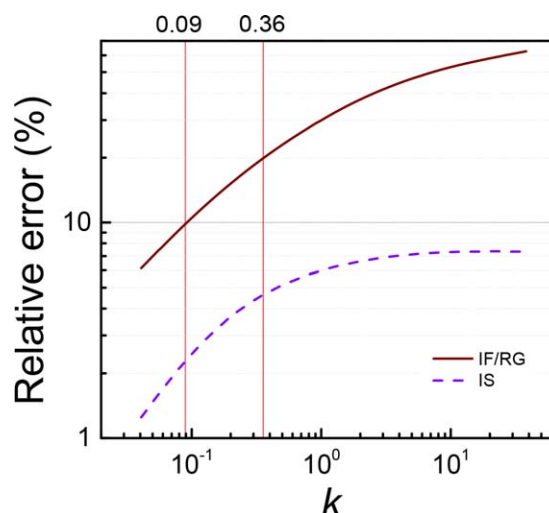


Figure 5. Relative errors of dissolution curves generated by approximations to numerical results.

[Color figure can be viewed at wileyonlinelibrary.com]

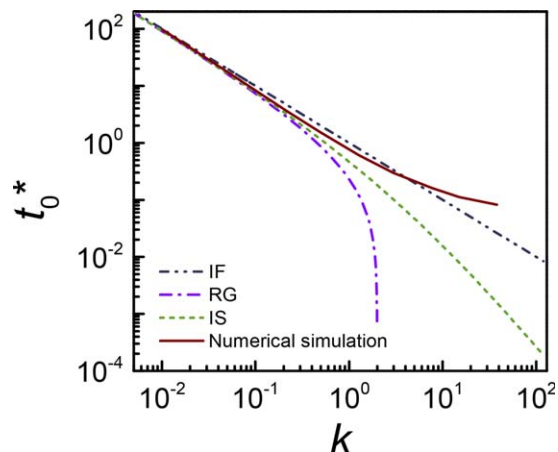


Figure 6. Normalized total dissolution time calculated using approximations and numerical solution from Ref. 12.

[Color figure can be viewed at wileyonlinelibrary.com]

The relative errors of the total dissolution time of the approximations to the numerical method are calculated and shown in Figure 7. It only shows the results for $k < 1$, a region with limited deviations. The deviation from the numerical simulation increases with k values. In the whole range considered, the relative error of IS is always smaller than that of RG. The relative error of the IF approximation is the smallest with $k < 0.02$ and that of IS approximation is smaller than those of the other two with $0.02 < k < \text{ca. } 0.7$.

Figure 7 can be served as a guideline for the applicable range of the approximations with respect to the total dissolution time. For instance, to control the error below 10%, IF is appropriate for $k < 0.03$, RG for $k < 0.06$, and IS for $k < 0.15$.

All three methods can merely be feasible for a limited range of k values. In fact, this is the intrinsic limitation of the approximate solutions due to the assumptions made to solve the problem.

The IF and IS approximations assume that the interface between the particle and the solution is fixed and the influence of interface motion on the diffusion field is ignored, which means

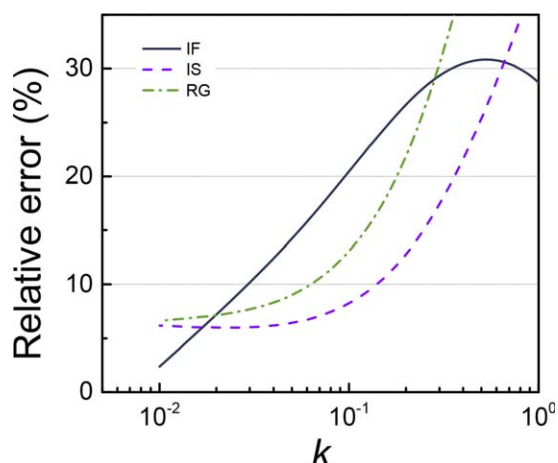


Figure 7. Relative errors of total dissolution time of approximated methods to numerical results.

[Color figure can be viewed at wileyonlinelibrary.com]

$$\frac{dR}{dt} \approx 0 \quad (23)$$

This will only be approached with reasonable accuracy when

$$(C_P - C_M) \gg (C_I - C_M) \quad (24)$$

which means

$$C_A = \frac{C_I - C_M}{C_P - C_M} \rightarrow 0 \quad (25)$$

where C_A is another saturation parameters.

Thus,

$$k \equiv \frac{2(C_I - C_M)}{C_P - C_I} = \frac{2C_A}{1 - C_A} \rightarrow 0 \quad (26)$$

In addition, the IF approximation treats the dissolution as a quasi-equilibrium process. This assumption is only true when k is extremely small. That is why both the IF and IS approximations are only suitable for conditions with small k and the application range (range of k values) for IF is even smaller than IS.

RG treats dissolution as essentially the reverse of growth. The solution comes from the exact solution for the growth of spherical precipitates and replaces the growth time t_g with $(\tau_{RG} - t)$. For growth, the concentration profile fulfills

$$D \left(\frac{\partial^2 C}{\partial r^2} + \frac{2}{r} \frac{\partial C}{\partial r} \right) = \frac{\partial C}{\partial t_g} \quad (27)$$

And

$$\frac{\partial C}{\partial t_g} = \frac{\partial C}{\partial t} \frac{d(\tau_{RG} - t)}{dt} = - \frac{\partial C}{\partial t} \quad (28)$$

Thus, for dissolution,

$$D \left(\frac{\partial^2 C}{\partial r^2} + \frac{2}{r} \frac{\partial C}{\partial r} \right) = - \frac{\partial C}{\partial t} \quad (29)$$

which suggests that the solution does not follow Fick's second law (Eq. 1) and deviates from describing dissolution exactly. Only when k is small and dissolution is slow, the change of concentration profile is accordingly slow

$$\frac{\partial C}{\partial t} \approx 0 \quad (30)$$

The deviation can be small and the solution has reasonable accuracy.

Another main source of these deviations should be ignoring the convection induced by density differences. Cable and Evans⁸ investigated the influence of convection due to the density difference between the two phases, i.e., the solute will not occupy the same volume in the solution as it does in the pure solute. The numerical simulation results⁸ showed that the influence is less than 10% up to $k = 1.0$, while the influence increases progressively important with increasing k .

Diffusion coefficient is a crucial parameter in a kinetics study. It can be calculated via total dissolution time τ , t_0^* , or t_0^* using Eqs. 10, 15, or 21. The data needed are the total dissolution time τ , original radius R_0 , and k . The first two can be obtained directly from experimental results and k from a simple calculation. The approximate method that estimates the dimensionless total dissolution time t_0^* best should also be the best option for the estimation of diffusion coefficient. It can be selected using Figure 7 with k values for given error levels.

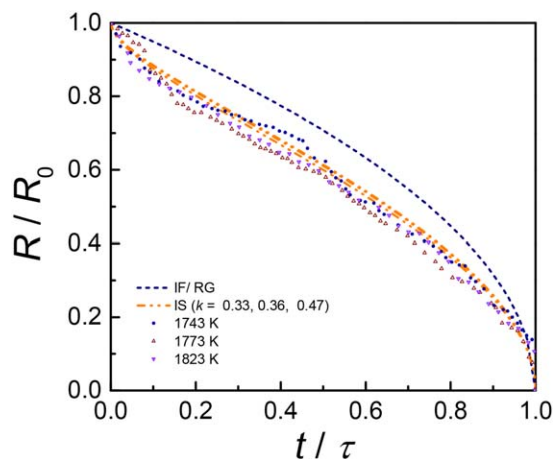


Figure 8. Experimental dissolution curves of Al_2O_3 particles in $\text{CaO-Al}_2\text{O}_3\text{-SiO}_2$ melt at different temperatures compared with different approximations.

[Color figure can be viewed at wileyonlinelibrary.com]

Figures 5 and 7 can be used as references when selecting an appropriate approximation taking into account experimental uncertainty and precise level desired. Generally speaking, the IS approximation can be considered to be the best estimation method for two reasons. First, the dissolution curves it produces (Figure 4) can reflect the influence of k and in good agreement with the numerical simulation results. The deviation is less than 8% for k up to 38 (Figure 5). Compared to the other two approximations, the IS approximation reaches the best estimate of the total dissolution time and the diffusion coefficient for $0.02 < k < 0.7$ and the relative error is less than 6% for $k < 0.02$. Conversely, the IF approximation needs the least calculation. It can be a good choice when k is extremely small and the error can be controlled well under the desired level. However, the applicable range of the approximations is limited and none of the approximations gives satisfactory results for large k values.

Applications on kinetics studies

*Dissolution of Alumina Particles in a $\text{CaO-Al}_2\text{O}_3\text{-SiO}_2$ Melt*¹⁵. To test the validity of the approximations, experimental data from our previous research¹⁵ are employed. The authors observed the dissolution behavior of spherical alumina particles in a $\text{CaO-Al}_2\text{O}_3\text{-SiO}_2$ melt using CSLM.¹⁵ The experimental setup was similar to that of this work. Another reason to choose Ref. 15 is that the diffusion coefficients at

different temperatures were obtained by combining the experimental observations and lattice Boltzmann model simulations. These data can serve as good references for the evaluation of the approximations.

Figure 8 shows the dissolution curves of Al_2O_3 particles in a $\text{CaO-Al}_2\text{O}_3\text{-SiO}_2$ melt at different temperatures. The curves exhibit slightly a "S" shape, indicating a faster dissolution rate at the beginning and at the end than that in the middle of the dissolution process. The parameters used to calculate the theoretical dissolution curves and diffusion coefficients are listed in Table 1. Since the differences among k values are relatively small, the dissolution curves calculated by the IS approximation are, just like the experimental points, close to each other for different temperatures. Therefore, only three representative experimental results are selected and shown in Figure 8. Since the values of k are around 0.3–0.5, as shown in Figure 5, the IS approximation can represent the dissolution processes best among the three approximations (error < 8%) and IF or RG approximation deviates considerably from the experimental results (error ca. 20%). The good agreement between the IS approximation and experimental data indicates that the dissolution of alumina particles in $\text{CaO-Al}_2\text{O}_3\text{-SiO}_2$ is diffusion controlled. If the experimental results are only compared with the theoretical line of IF or RG, it may exclude diffusion as a rate controlling step.

The particle radius and total dissolution time of each experiment are listed in Table 2. The diffusion coefficients, as well as the activation energy estimated with these approximations, can also be found in Table 2. The physicochemical parameters used in the calculations are listed in Table 1. Rather significant variations can be noticed among different approximations for both the diffusion coefficients and activation energy. As shown in Figure 7, the deviation can be as high as 30% for $k = 0.6$. The relative errors of the diffusion coefficients obtained via the three approximations to the numerical results (given in Table 2) are shown in Figure 9. Even though the values estimated with the IS approximation are those closest to the simulation results, some of the relative error are still larger than 10% (Figure 9).

As stated in the article,¹⁵ the reproducibility was rather satisfied at 1743 and 1773 K. Increase in scattering was observed at higher temperatures, i.e., 1823, 1873, and 1903 K in the study.¹⁵ The relative errors of the experiments at different temperatures were calculated based on the deviation of total dissolution time and are listed in Table 3. Most of them are well below 10 % except for 1903 K. According to Figure 7, even for IS, the relative error is around 20~30% for $k = 0.33\sim 0.66$. This suggests that none of the approximation

Table 1. Parameters Used for Calculating Theoretical Dissolution Curves and Diffusion Coefficients

System	Temperature (K)	C_1 (mol/L)	C_M (mol/L)	C_p (mol/L)	k	p	λ_R
Al_2O_3	1743	9.6 ^a	5.6	34 ^c	0.33	0.16	0.40
	1773	9.9 ^a	5.6	34 ^c	0.36	0.17	0.42
	1823	11 ^a	5.6	34 ^c	0.47	0.19	0.51
	1873	12 ^a	5.6	34 ^c	0.59	0.22	0.62
	1903	13 ^a	5.6	34 ^c	0.66	0.23	0.68
Nd_2O_3	1141	7.6×10^{-2b}	0	20 ^d	7.5×10^{-3}	2.5×10^{-2}	4.5×10^{-2}
	1191	7.5×10^{-2b}	0	20 ^d	7.5×10^{-3}	2.4×10^{-2}	4.5×10^{-2}
	1241	7.4×10^{-2b}	0	20 ^d	7.4×10^{-3}	2.4×10^{-2}	4.5×10^{-2}
	1291	7.3×10^{-2b}	0	20 ^d	7.3×10^{-3}	2.4×10^{-2}	4.4×10^{-2}

^aThe saturated concentration was obtained from Refs. 3 and 15, and the density of the melt was calculated according to the data from Ref. 21.

^bThe solubility was obtained from Ref. 22, and the density of the melt was calculated according to the data from Ref. 18.

^cThe porosity of the particles is assumed to be the same as the Nd_2O_3 particles made for this study, which is 11%.

^dThe apparent density was measured by the Archimedes' method.

Table 2. Diffusion Coefficients Obtained via Different Approximations

System	Temperature (K)	R_0 (μm)	τ (s)	D ($10^{-6}\text{cm}^2/\text{s}$)				E (10^2kJ/mol)		
				IF	IS	RG	Simulation	IF	IS	RG
Al_2O_3	1743	250	4450	0.43	0.27	0.22	0.24 ^a	2.8	2.4	3.2
	1743	250	4200	0.45	0.28	0.24	0.25 ^a			
	1773	250	3800	0.46	0.29	0.24	0.26 ^a			
	1773	250	3580	0.49	0.30	0.25	0.28 ^a			
	1823	250	2160	0.62	0.36	0.28	0.33 ^a			
	1823	250	1950	0.69	0.40	0.31	0.34 ^a			
	1823	250	1825	0.74	0.43	0.33	0.38 ^a			
	1873	250	1280	0.83	0.45	0.32	0.42 ^a			
	1873	250	1200	0.88	0.48	0.34	0.48 ^a			
	1873	250	1340	0.79	0.43	0.31	0.41 ^a			
	1903	250	550	1.7	0.92	0.61	0.84 ^a			
	1903	250	470	2.0	1.1	0.72	0.97 ^a			
	1903	250	720	1.3	0.70	0.47	0.69 ^a			
	1903	250	740	1.3	0.68	0.46	0.66 ^a			
	Nd_2O_3	1141	292	7371	15	14	14			
1191		297	5550	21	20	20	–			
1241		169	810	48	44	44	–			
1291		323	2263	63	59	58	–			

^aData are taken from Ref. 15.

should be applied for estimating diffusion coefficients due to possible large deviation. Numerical simulation has to be employed.

Dissolution of Nd_2O_3 Particles in a $\text{LiF}\text{-}24\text{CaF}_2$ Melt.

Figure 10 shows the dissolution curves of Nd_2O_3 particles in $\text{LiF}\text{-}24\text{CaF}_2$ melt at different temperatures. The parameters used to generate the theoretical lines are listed in Table 1. Similarly, as the k values are very close to each other, the theoretical lines calculated via the IS approximation are hard to be distinguished. The differences among IF, RG, and IS are also small. Figure 5 suggests that the deviation of the dissolution curves of IF, RG, and IS from the numerical simulation is well

below 10% for $k = \text{ca. } 0.007$. Any of the three approximations is feasible to verify the controlling step. The IF or RG approximation (Eqs. 9 and 14) has a simpler form and is easier to generate the theoretical curve than the IS approximation. The experimental data at these temperatures are also shown in Figure 10, which match the theoretical lines quite well. This suggests that the rate controlling step of dissolution is the diffusion of Nd_2O_3 in $\text{LiF}\text{-}24\text{CaF}_2$ melt.

The diffusion coefficients estimated with these models are also listed in Table 2. As discussed previously in section “Evaluation of Approximations”, the variation among different approximations is negligible with respect to the experimental uncertainty, since the k values are small. The variation of the diffusion coefficients estimated by IF, IS, and RG is less than 10% as expected (Table 2). The activation energy is calculated to be 1.2×10^2 kJ/mol for all three approximations. This further indicates that any of the three approximations can fulfill the accuracy requirements. The IF approximation would be recommended here as its solution is the simplest and

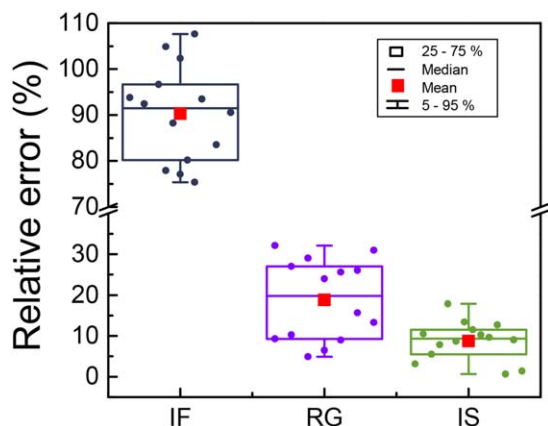


Figure 9. Relative errors of diffusion coefficients obtained by approximations compared to numerical results.

[Color figure can be viewed at wileyonlinelibrary.com]

Table 3. Relative Errors of the Experiments at Different Temperatures

Temperature (K)	1743	1773	1823	1873	1903
Relative error (%) ^a	4	4	9	6	21

^aBased on the total dissolution time of the experiments conducted at each temperature.

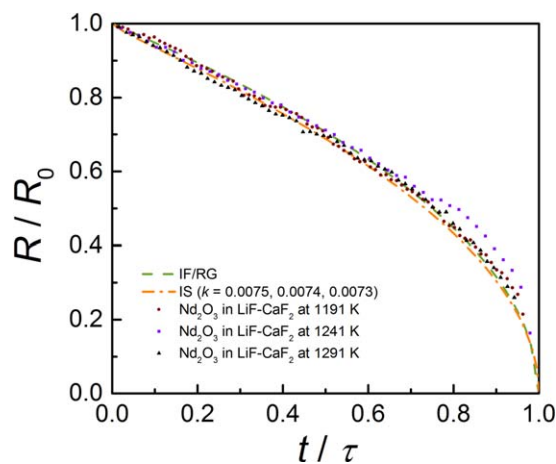


Figure 10. Dissolution curves of Nd_2O_3 particles in molten $\text{LiF}\text{-}\text{CaF}_2$ at different temperatures compared with different models.

[Color figure can be viewed at wileyonlinelibrary.com]

explicit, and there is no need to solve the implicit Eqs. 13 or 20.

Conclusions

This research provides a systematic evaluation and the applications in real practices of three approximations, i.e., IF, RG, and IS approximations, describing the diffusion-limited dissolution of a spherical particle in an infinite medium. The conclusions can be given as follows:

1. Considering both the generated dissolution curves and estimated diffusion coefficient, the IS approximation can be considered to be the best estimation method among the three with $k < 0.7$. All the three approximations can only be applied with limited k values to obtain satisfactory results. Figures 5 and 7 are the guidelines for determining the applicable ranges.

2. The IF and RG approximations have the identical dissolution curves independent of k and are only feasible for small k , e.g., $k < 0.09$ with error $< 10\%$, or $k < 0.4$ with error $< 20\%$. By contrast, the dissolution curves produced by the IS approximation can reflect the influence of k and agrees well with the numerical simulation results. The deviation is less than 8% for k up to 38.

3. Estimating total dissolution time, the three approximations can merely be feasible for small k values. The IF approximation is the best with $k < 0.02$ and IS approximation is better than the other two with $0.02 < k < \text{ca. } 0.7$. For all three approximations, the relative errors are larger than 10% with $k > 0.15$.

4. The dissolution of alumina particles in CaO-Al₂O₃-SiO₂ is diffusion controlled. The IS approximation can represent the dissolution processes well. With $k = 0.33 \sim 0.66$, the deviation of estimated diffusion coefficients by the approximations may be as high as 30%. None of the approximation is appropriate for this purpose.

5. The rate controlling step of the dissolution of Nd₂O₃ in LiF-24CaF₂ is also the diffusion of solute in the melt. The differences among the three approximations can be neglected as for $k = 0.0073 \sim 0.0075$. Any of them can reproduce the experimental data with satisfied agreement. The errors of the diffusion coefficients obtained should be well below 10%.

Acknowledgments

The authors thank Dr. Abhishek Mukherjee for his generous help in the CSLM experiments. The authors would like to acknowledge the EU FP7 project REEcover (Project ID: 603564) for financial support of this study and CAS Pioneer Hundred Talents Program for supporting the work from Dr. Zhi Sun.

Literature Cited

1. Agren J. Kinetics of carbide dissolution. *Scand J Metall.* 1990;19(1): 2–8.
2. Costa P, Sousa Lobo JM. Modeling and comparison of dissolution profiles. *Eur J Pharm Sci.* 2001;13(2):123–133.
3. Guo X, Sun Z, Van Dyck J, Guo M, Blanpain B. In-situ observation on lime dissolution in molten metallurgical slags-kinetic aspects. *Ind Eng Chem Res.* 2014;53(15):6325–6333.
4. Levenspiel O. *Chemical Reaction Engineering*, 3rd ed. New York: Wiley, 1999.
5. Aaron H, Kotler G. Second phase dissolution. *Metall Trans.* 1971; 2(2):393–408.
6. Aaron HB, Fainstei D, Kotler GR. Diffusion-limited phase transformations - a comparison and critical evaluation of mathematical approximations. *J Appl Phys.* 1970;41(11):4404.
7. Readey DW, Copper AR. Molecular diffusion with a moving boundary and spherical symmetry. *Chem Eng Sci.* 1966;21(10):917–922.
8. Cable M, Evans DJ. Spherically symmetrical diffusion-controlled growth or dissolution of a sphere. *J Appl Phys.* 1967;38(7):2899.
9. Tundal UH, Ryum N. Dissolution of particles in binary-alloys.1. Computer-simulations. *Metall Mater Trans A.* 1992; 23(2):433–444.
10. Nojiri N, Enomoto M. Diffusion-controlled dissolution of a spherical precipitate in an infinite binary alloy. *Scr Metall Mater.* 1995;32(5): 787–791.
11. Verhaeghe F, Arnout S, Blanpain B, Wollants P. Lattice-Boltzmann modeling of dissolution phenomena. *Phys Rev E.* 2006;73(3):10.
12. Brown LC. Diffusion-controlled dissolution of planar, cylindrical, and spherical precipitates. *J Appl Phys.* 1976;47(2):449–458.
13. Sridhar S, Cramb AW. Kinetics of Al₂O₃ dissolution in CaO-MgO-SiO₂-Al₂O₃ slags: in situ observations and analysis. *Metall Mater Trans B.* 2000;31(2):406–410.
14. Liu J, Guo M, Jones PT, Verhaeghe F, Blanpain B, Wollants P. In situ observation of the direct and indirect dissolution of MgO particles in CaO-Al₂O₃-SiO₂-based slags. *J Eur Ceram Soc.* 2007;27(4): 1961–1972.
15. Liu J, Verhaeghe F, Guo M, Blanpain B, Wollants P. In situ observation of the dissolution of spherical alumina particles in CaO-Al₂O₃-SiO₂ melts. *J Am Ceram Soc.* 2007;90(12):3818–3824.
16. Sun ZHI, Guo X, Van Dyck J, Guo M, Blanpain B. Phase evolution and nature of oxide dissolution in metallurgical slags. *AIChE J.* 2013;59(8):2907–2916.
17. Perry DL. *Handbook of Inorganic Compounds*, 2nd ed. Boca Raton, FL: CRC Press, Taylor & Francis Group, 2011.
18. Porter B, Meaker RE. *Density and Molar Volumes of Binary Fluoride Mixtures*. US: Department of the Interior, Bureau of Mines, 1966.
19. Brown LC. Shape changes during dissolution of theta-CuAl₂. *Metall Mater Trans A.* 1984;15(3):449–458.
20. Whelan MJ. On the kinetics of precipitate dissolution. *Metal Sci.* 1969;3(1):95–97.
21. Bottinga Y, Weill DF. Densities of liquid silicate systems calculated from partial molar volumes of oxide components. *Am J Sci.* 1970; 269(2):169.
22. Guo X, Sun Z, Sietsma J, Yang Y. Semiempirical model for the solubility of rare earth oxides in molten fluorides. *Ind Eng Chem Res.* 2016;55(16):4773–4781.

Manuscript received Sep. 16, 2016, and revision received Jan. 4, 2017.